Research Article

Shaik Mohammad Altaff, Tiruveedula Raja Rajeswari*, and Chennamsetty Subramanyam

In silico ADMET, molecular docking study, and nano Sb_2O_3-catalyzed microwave-mediated synthesis of new α-aminophosphonates as potential anti-diabetic agents

https://doi.org/10.1515/mgmc-2022-0023
received November 27, 2021; accepted August 23, 2022

Abstract: An efficient and greener method is developed for the synthesis of *α*-aminophosphonates *via* Kabachnik–Fields reaction in solvent free condition using microwave irradiation technique. For all of the compounds, an *in silico* ADMET and molecular docking study was conducted to get insight on the drug likeliness behavior as well as their ability to block the enzyme *α*-amylase. The compounds with significant binding affinity and significant pharmacokinetic characteristics were produced. The newly produced compounds were spectroscopically analyzed to confirm their structure, and *in vitro* α-amylase inhibitory activity was also tested for all of them. The compounds **8j** (half-maximal inhibitory concentration (IC_{50}), 100.5 ± 0.2 μg·mL^{-1}) showed better inhibitory activity than the reference drug, acarbose. The compounds **8d** (IC_{50}, 108.6 ± 0.2 μg·mL^{-1}), **8g** (IC_{50}, 110.9 ± 0.3 μg·mL^{-1}), **8h** (IC_{50}, 115.0 ± 0.1 μg·mL^{-1}), and **8f** (IC_{50}, 118.9 ± 0.2 μg·mL^{-1}) have been reported to exhibit significant inhibition toward the target enzyme. All the leftover compounds displayed modest to excellent inhibition through IC_{50} values in the range from 122.3 ± 0.3 to 154.3 ± 0.6 μg·mL^{-1} while comparing with the reference drug, Acarbose (IC_{50}, 103.2 ± 0.7 μg·mL^{-1}). The results disclosed that the majority of these compounds exhibit significant α-amylase inhibitory activity.

Keywords: α-aminophosphonates, Kabachnik–Fields reaction, microwave irradiation, molecular docking, α-amylase

*** Corresponding author: Tiruveedula Raja Rajeswari,** Sri A.S.N.M. Government College (Autonomous), Palakol, AP-534260, India, e-mail: rajarajeswarit865@gmail.com
Shaik Mohammad Altaff: Department of Chemistry, S.N. Government Junior College, Chebrole, AP-522212, India
Chennamsetty Subramanyam: Department of Chemistry, Bapatla Engineering College, Bapatla, AP-522101, India

1 Introduction

Organophosphorus compounds have gained significance in industrial, agricultural, medicinal, and synthetic organic chemistry as a result of their distinct physical, chemical, and biological properties (Bagi et al., 2019; Basha et al., 2016; Jean-Luc, 2014; Shameem and Orthaber, 2016). α-Aminophosphonates (α-Aps), for instance, are an intriguing class of bioactive analogues that mimic active peptide transition states and have features similar to naturally occurring amino acids (Orsini et al., 2010). α-Aps possess broad range of applications in the field of medicine (Mucha et al., 2011, Naydenova et al., 2010), biology (Smith and Bartlett, 1998), and industry (Dhawan and Redmore, 1987). They are useful compounds as antibiotics (Hirschmann et al., 1994; Kuemin and Donk, 2010), fungicides (Yang et al., 2006), bactericides (Herczegh et al., 2002), herbicides (Maier, 1990), enzyme inhibitors (Allen et al., 1989), antitumor reagents (Huang et al., 2013; Kafarski and Lejczak, 2001), anti-cancer agents (Bhattacharya et al., 2013), anti-thrombotic agents (Meyer and Barlett, 1998), anti-inflammatory (Damiche and Chafaa, 2017; Sujatha et al., 2017), anti-oxidants (Mohan et al., 2016), antiviral agents (Xie et al., 2017), protease inhibitors (Miller et al., 1998), peptide mimetics (Natchev, 1988), glutamine synthetase (Bayer et al., 1972), plant growth regulators (Maheshwara Reddy et al., 2021), metal corrosion preventor (Kuznetsov et al., 2003), and anti-diabetic agents (Madhu Kumar Reddy et al., 2021).

The nucleophilic addition of phosphites to imines, i.e., the Kabachnik–Fields (K–F) reaction, was shown to be a convenient approach among the several synthetic processes proposed for the synthesis of α-Aps (Ordonez et al., 2009). Several papers have recently been published describing the synthesis of α-Aps employing Lewis acids (Ghafuri et al., 2016; Ghosh et al., 2004; Tang et al., 2011; Wang et al., 2015), Bronsted acids (Farahani and Akbari, 2017; Mitragotri et al., 2008; Mohammadiyan et al., 2017;

Rostamizadeh et al., 2011; Vahdat et al., 2008), solid acids (Sreekanth Reddy et al., 2014), bases (Lewkowski et al., 2014; Motevalli et al., 2015), nano catalysts (Kaboudin et al., 2017; Ravikumar et al., 2018; Syama Sundar et al., 2014), and other catalysts in the K–F reaction (Azaam et al., 2018; Karimi-Jaberi and Amiri, 2010; Ningbo et al., 2014; Yu and Xu, 2015). Although these methods are suitable for the one-pot synthesis of α-Aps, they have at least one disadvantage, such as extended reaction periods, low product yields requiring stoichiometric concentrations of catalysts, excess phosphorus compounds, or the usage of additives.

Oxides of antimony (OA) play a key role among all the other metal oxides from V to VI groups in the field of chemical, sensing, and semiconductors (Brebua et al., 2007; Dzimitrowicz et al., 1982; Laachachi et al., 2004; Nalin et al., 2001; Ozawa et al., 1998; Xie et al., 2004). In comparison to bulk OA, literature shows that nanoparticles of OA have superior qualities, such as a higher refractive index (Nalin et al., 2001), stronger abrasion resistance, higher proton conductivity (Dzimitrowicz et al., 1982; Ozawa et al., 1998), excellent mechanical strength (Chang et al., 2009), and higher absorbability (Xie et al., 1999). They possess a remarkable catalytic property in poly(ethylene terephthalate) and organic synthesis industries (Duh, 2002; Matsumura et al., 2006; Nanda et al., 2002; Spengler et al., 2001). Especially, nano Sb_2O_3 possess low affinity to side products, easy recovery, insoluble in organic solvents, avoids unwanted color, and acts as a catalytic agent in organic synthesis (Liu and Iwasawa, 2002). Recently, it has been reported that nano Sb_2O_3 can be effective in the synthesis of α-Aps (Syamala, 2009).

On the other hand, microwave (MW) irradiation (Mohan et al., 2016) provided a new approach of energizing the reaction mixture since it involves the direct transfer of energy to the substrate molecules and will boost the rate of the reaction by rapid kinetic excitation of molecules. MW-assisted organic syntheses have attracted a lot of attention from chemists in recent years because of their benefits such as shorter reaction times, cleaner products, operational simplicity, higher yields, and the possibility of achieving effective synthesis of heterocyclic bioactive compounds (De la Hoz et al., 2005; Sujatha et al., 2017). The use of a solvent-free reaction state has been shown to be an effective method for a variety of chemical reactions (Tanaka, 2000). This is a perfect platform for the three components of the K–F reaction, which may all be done in one pot.

In the disciplines of medical, drug design, and agrochemicals, dyes, photochemistry, and combinatorial chemistry, molecules with heterocyclic ring structures have attracted a lot of interest (Shiro et al., 2015; Vorathavorn et al., 2013). Thiazolidinediones (TZDs) are a type of heterocyclic molecule having a wide range of biological functions (Angajala et al., 2014; Bozdag-Dündar et al., 2008; Ceriello, 2008; Eun et al., 2007; Mori et al., 2008; Sahu et al., 2007). TZDs are being used to treat a variety of diabetic problems in type 2 diabetes mellitus patients (Yoshioka et al., 1989). Our recent study demonstrated that organophosphorus compounds bearing TZD moiety would be effective as α-amylase and α-glucosidase inhibitors in the diabetic treatment (Altaff et al., 2021; Hidalgo-Figueroa et al., 2013; Ibrar et al., 2017; Kaur et al., 2018; Pavan Phani Kumar et al., 2021; Ramandeep et al., 2021; Senthil et al., 2019; Sujatha et al., 2020; Vijay et al., 2022; Wang et al., 2017). By considering the above facts and in continuation of our studies toward developing new methods for the synthesis of bioactive α-Aps (Haji basha et al., 2020; Ravikumar et al., 2018; Subramanyam et al., 2017; Sujatha et al., 2017), we decided to explore the possibility of implementing a MW-mediated one-pot three-component reaction for the preparation of α-Aps using nano Sb_2O_3 as catalyst under solvent-free condition.

2 Results and discussion

2.1 Chemistry

In the present work, we have designed and synthesized a series of α-Aps (**8a–j**) starting with 2,4-thiazolidine-dione with good yields (89–95%). The synthetic strategy of α-Aps (**8a–j**) is presented in Scheme 1.

Initially, a model reaction was carried out for this reaction involving a mixture of picolinaldehyde (**6a**), diethyl (4-(2,4-dichlorophenyl)thiazol-2-ylamino)(phenyl) methyl-phosphonate (**5**), and diethyl phosphite (**7**). At the beginning of investigation, the reaction was carried out using tetrahydrofuran (THF) as solvent at 40°C without using any catalyst. In this case, the model molecules were not able to undergo efficient reaction to give the desired product, diethyl (4-((*E*)-(2,4-dioxothiazolidin-5-ylidene)methyl)phenylamino)(pyridin-2-yl)methylphosphonate (**8a**), and obtained very poor yield (30%) of the product (Table 1, entry 1). Then, the reaction was carried out in the presence of a catalyst. In search for an efficient catalyst, the model reaction was conducted using catalyst (10 mol%) such as $NiBr_2$, $ZnCl_2$, $LaCl_3$, $CuCl_2$, $AlCl_3$, and $BF_3{\cdot}Et_2O$. The results are presented in Table 1 (entries 2–7).

It was observed that the yield of the product **8a** was improved from 30% to the range of 59–69%, indicating

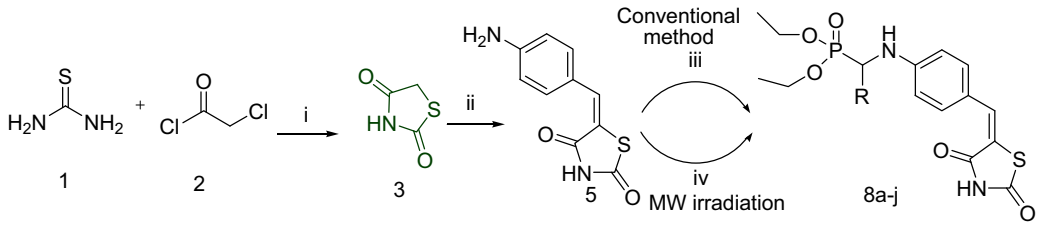

i).H2O, r.t. ii) p-aminobenzaldehyde (4), pyperidine, toluene, r.t.;iii).Nano Sb_2O_3, THF, R-CHO (6a-j), diethyl phosphonate (7), 40 ^{0}C; iv) Nano Sb_2O_3, MW, R-CHO (6a-j), diethyl phosphite (7)

Compd	8a	8b	8c	8d	8e
R	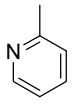	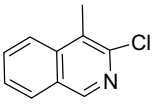	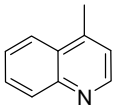	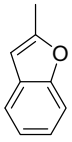	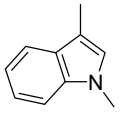
Compd	8f	8g	8h	8i	8j
R	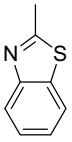	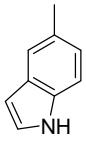	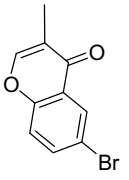	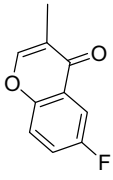	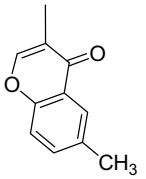

Scheme 1: Microwave-assisted synthesis of α-Aps (**8a–j**).

Table 1: Synthesis of compound **8a** under various conditions[a]

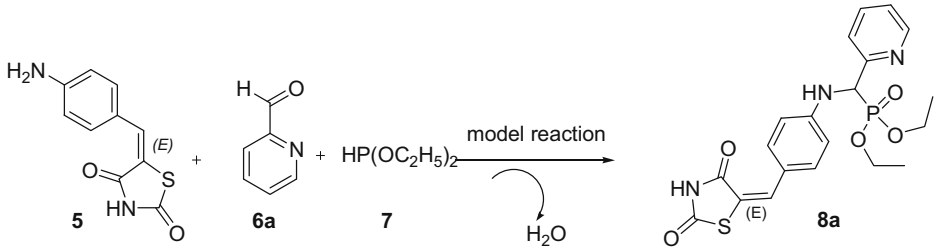

Entry	Catalyst (mol%)	Solvent	Temp. (°C)	Time	Yield[b] (%)
1	—	THF	40	24 h	30
2	$NiBr_2$ (10)	THF	40	7 h	59
3	$ZnCl_2$ (10)	THF	40	6 h	63
4	$LaCl_3$ (10)	THF	40	6 h	60
5	$CuCl_2$ (10)	THF	40	5 h	65
6	$AlCl_3$ (10)	THF	40	5 h	60
7	$BF_3{\cdot}Et_2O$ (10)	THF	40	4.5 h	69
8	Nano Sb_2O_3 (10)	THF	40	3 h	78
9	Nano Sb_2O_3 (10)	DCM	40	3.5 h	73
10	Nano Sb_2O_3 (10)	Toluene	60	4 h	70
11	Nano Sb_2O_3 (10)	Ethanol	40	3.5 h	71
12	Nano Sb_2O_3 (10)	Solvent-free	40	2 h	89
13	Nano Sb_2O_3 (10)	Solvent-free (MW)	Room temp.	15 min	93

[a]Reaction of picolinaldehyde, diethyl (4-(2,4-dichlorophenyl)thiazol-2-ylamino)(phenyl)methyl-phosphonate and diethyl phosphite were selected as models to optimize reaction conditions.
[b]Isolated yield.

that the catalyst plays a hopeful role in the process. On the other hand, OA especially, nano Sb_2O_3, play a key role as catalytic agent in organic synthesis. Hence, nano Sb_2O_3 (10 mol%) was utilized in the model reaction to prepare compound **8a**. A good yield (78%) (Table 1, entry 8) of the compound **8a** was obtained, when THF was used as solvent within 3 h. Additionally, the effect of solvent on the reaction was also analyzed by varying different solvents such as dichloromethane (DCM), toluene, and ethanol. No appreciable yield of the product (70–73%) was found (Table 1, entry 9–11). Then, we tried this reaction without solvent. In this case, a good yield (89%) of the product was obtained within 2 h (Table 1, entry 12). Further, to improve the reaction conditions and to reduce the time to complete the reaction, the reaction mixture was MW-irradiated (450 W) without solvent using nano Sb_2O_3 (10 mol%). In this case, we obtained better yield (93%) of **8a** within 10 min (Table 1, entry 13).

Further, the role of catalyst amount (nano Sb_2O_3) on the model reaction was also studied with different catalyst amounts ranging from 1 to 12.5 mol% (Table 2, entry 1–6). But no appreciable yield of the compound **8a** other than 10 mol% was found. Hence, 10 mol% of the catalyst was confirmed using MW irradiation under solvent-free situation. The obtained results are summarized in Table 2. The reusability of nano Sb_2O_3 (10 mol%) was also studied. The product was filtered and the residue was washed with chloroform after every run to take away stains from surface of the catalyst and then reused it up to five times to prepare compound **8a** (Table 3, entry 1–5). Hence, nano Sb_2O_3 (10 mol%) might efficiently catalyze the reaction without solvent under MW irradiation.

Once the reaction conditions were optimized, the generality of this process to synthesize α-Aps (**8b**–**j**) (Scheme 1) was studied with numerous aldehydes (**6b**–**j**), amine (**5**), and diethyl phosphite (**7**) in the presence of nano Sb_2O_3 (10 mol%) without solvent using MWI technique and Table 4 depicted the summary of results of this study. The detailed mechanism to synthesize new α-Aps (**8a**–**j**) is presented in Figure S1. Initially the carbonyl group of aldehyde reacts with amine to form an intermediate imine (A). The activated intermediate imine then reacts with diethylphosphite to give the respective α-Aps (**8a**–**j**).

Table 2: The effect of the amount of catalyst, Nano Sb_2O_3 (10 mol%), to promote the Kabachnik–Fields reaction[a]

Entry	Amount of catalyst (mol%)	Time (min)	Yield[b] (%)
1	1	15	60
2	2.5	15	64
3	5	15	69
4	7.5	15	80
5	10	15	93
6	12.5	15	92

[a]Reaction of picolinaldehyde, diethyl (4-(2,4-dichlorophenyl) thiazol-2-ylamino)(phenyl)methyl-phosphonate and diethyl phosphite were selected as models to optimize reaction conditions.
[b]Isolated yield.

Table 3: Reusability of the catalyst, nano Sb_2O_3 (10 mol%), for the synthesis of compound 5a[a]

Entry	Nano Sb_2O_3 (10 mol%)	Time (min)	Yield[b] (%)
1	1st run	15	93
2	2nd run	15	92
3	3rd run	15	90
4	4th run	15	89
5	5th run	15	83

[a]Reaction of picolinaldehyde, diethyl (4-(2,4-dichlorophenyl) thiazol-2-ylamino)(phenyl)methyl-phosphonate and diethyl phosphite were selected as models to optimize reaction conditions.
[b]Isolated yield.

Nuclear magnetic resonance (NMR) (^{31}P, ^{1}H, ^{13}C), infrared (IR) spectroscopy, mass, and elemental studies were used to confirm the structures of the newly synthesized compounds **8a**–**j**. For the compounds **8a**–**j**, singlet ^{31}P NMR signals were found in the range of 25.3–15.7 ppm (Altaff et al., 2021; Quin et al., 1994). The signal attributable to the N–H proton of the thiazolidinedione ring and the NH proton linked to the phenyl ring were seen at 11.52 and 5.71 ppm for **8a**–**j** in their ^{1}H-NMR spectra. The aromatic protons of **8a**–**j** produced two doublets at 7.02 and 6.33 ppm. The proton signals of compounds **8a**–**j** emerged as multiplets for methylene protons at 4.19 ppm and as triplets for methyl protons at 1.21 ppm. The signal for ethylene and methine proton was found at 7.12 and 3.90 ppm, respectively. In ^{13}C NMR spectra, the chemical shifts for carbonyl, ethylene, methylene, and methyl carbons were found at 165.8–164.5, 141.3, 63.5, and 13.7 ppm, respectively, in compounds **8a**–**j**. The remaining carbons' chemical changes were observed within their respective ranges. An IR spectral investigation of the prepared compounds was conducted in order to confirm their functional groups. In IR spectra, the absorption band in the range of 3,372–3,136 cm^{-1} is assigned to secondary amines of the compounds 8**a**–**j**. The stretching vibrations for P═O and P–O–C_{alip} were noticed at 1,221–1,210 and 1,012–1,004 cm^{-1}, respectively. M+ ions were found as base peaks in all the title compounds, as well as isotopic cluster peaks with the predicted ratio. The estimated elemental analysis values for the synthesized compounds were quite close to the empirical values. The Supplementary Materials contained typical spectra

Table 4: MW-mediated synthesis of α-aminophosphonates (**8a–j**)[a]

Compound	Aldehyde	Time (min)	Yield[b] (%)	Compound	Aldehyde	Time (min)	Yield[b] (%)
8a		10	93	**8f**	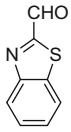	10	95
8b	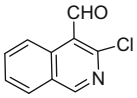	13	92	**8g**	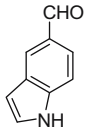	12	93
8c	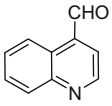	12	94	**8h**	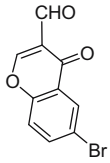	10	94
8d	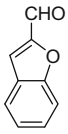	15	90	**8i**	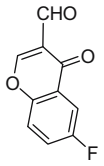	15	96
8e	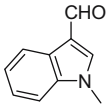	11	92	**8j**	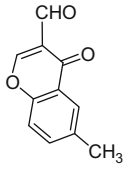	10	92

[a]Reaction of substituted aldehyde, diethyl (4-(2,4-dichlorophenyl)thiazol-2-ylamino)(phenyl)methyl-phosphonate and diethyl phosphite in the presence of nano Sb_2O_3 (10 mol%) without solvent under MWI.
[b]Isolated yield.

(^{1}H, ^{31}P, ^{13}C NMR, IR, mass, and CHN analyses) of compound **8a** as representative of title compounds (Figures S2–S7).

2.2 Pharmacology

2.2.1 *In silico* ADME analysis

In the process of drug discovery and development, compounds with high bioactivity and low toxicity are likely to be favored. One of the best ways to design new drug candidates is to use *in silico* ADMET (absorption, distribution, metabolism, excretion, and toxicity) property screening based on molecular structure. The rate of pharmacokinetic failure in clinical stages during the discovery phase is greatly reduced when ADME features are predicted early in the drug development process (Hay et al., 2014). SwissADME, which can be found at http://www.swissadme.ch, was used to test the ADME parameters of the proposed compounds. The prediction was based on the moieties' physicochemical and structural advantages. The physicochemical parameters of the molecules **8a–j** are displayed in Table 5 (molecular weight, heavy atoms, aromatic heavy atoms, ratio of sp^3 hybridized carbons over the total carbon number of the molecule, rotatable bonds, H-bond acceptors and donors, molar refractivity, lipophilicity, and water solubility). When compared to Acarbose, these metrics were in good agreement with the applied criteria for all the compounds **8a–j** and exhibited a good bioavailability score. The ADME parameters of the newly developed compounds are shown in Table 6. The gastrointestinal (GI) absorption of all the compounds was found to be minimal. Both passive blood–brain barrier (BBB) permeability and human gastrointestinal absorption (HIA) are demonstrated in the BOILED-Egg model's output (Daina and Zoete, 2016) (Figure S8). The reference drug, acarbose was found to be out of range and all the tested molecules were discovered outside the egg, indicating that they were not absorbed and hence were not BBB permeant. Knowledge of compounds that are non-substrate or substrate of the permeability glycoprotein

Table 5: Physicochemical properties of compounds **8a–j**

Compound	[a]MW	Heavy atoms	Aromatic heavy atoms	[b]Fraction C sp^3	Rotatable bonds	H-bond acceptors	H-bond donors	[c]MR	[d]TPSA	[e]iLOGP	[f]Silicos-IT class
8a	447.44	30	12	0.25	9	6	2	120.78	141.73	2.87	Poorly soluble
8b	531.95	35	16	0.21	9	6	2	143.29	141.73	3.44	Poorly soluble
8c	497.5	34	16	0.21	9	6	2	138.28	141.73	3	Poorly soluble
8d	486.48	33	15	0.22	9	6	2	132.76	141.98	3.28	Poorly soluble
8e	499.52	34	15	0.25	9	5	2	139.74	133.77	3.26	Poorly soluble
8f	503.53	33	15	0.23	9	6	2	136.16	169.97	3.45	Poorly soluble
8g	485.49	33	15	0.22	9	5	3	134.84	144.63	2.64	Poorly soluble
8h	593.38	36	16	0.21	9	7	2	146.73	159.05	3.58	Poorly soluble
8i	532.48	36	16	0.21	9	8	2	138.98	159.05	3.48	Poorly soluble
8j	528.51	36	16	0.24	9	7	2	143.99	159.05	3.37	Poorly soluble
Acarbose	645.6	44	0	0.92	9	19	14	136.69	321.17	0.63	Soluble

[a]Molecular weight; [b]The ratio of sp^3 hybridized carbons over the total carbon count of the molecule; [c]Molar refractivity; [d]topological polar surface area (Å^2); [e]lipophilicity; [f]water solubility (SILICOS-IT).

(Pgp) is used to evaluate the active efflux in biological membranes, especially for incidence from the GI wall to the lumen (Montanari and Ecker, 2015). Molecules 1 (**8a**) and 7 (**8g**) (Pgp–, blue dots) were anticipated to be effluated from the central nervous system by the Pgp, whereas molecules 2 (**8b**), 3 (**8c**), 4 (**8d**), 5 (**8e**), 6 (**8f**), 8 (**8h**), and 10 (**8j**) (Pgp+, red dots) were predicted not to be effluated.

In a pharmacokinetic study, it is crucial to forecast if a chemical will cause significant drug interactions by inhibiting cytochromes (CYPs) such CYP1A2, CYP2C19, CYP2C9, CYP2D6, and CYP3A4, as well as which isoenzymes would be affected (Hollenberg, 2002; Huang et al., 2008). Except **8f**, all other molecules were non-inhibitors of CYP1A2. The molecules 8a and 8e were found to be inhibitors of CYP2D6. The study further demonstrated that all the tested molecules were inhibitors of CYP2C19, CYP2C9, and CYP3A4. All these isoenzymes were shown to be non-inhibitors by the reference drug, acarbose. All the compounds had significant low skin permeability with high skin permeability coefficient (log *Kp*) values, with the reference medication having the least skin permeability and the highest log *Kp* of all the molecules examined (–16.29).

Predicting drug-likeness factors can aid qualitative identification of a compound that turns out to be an oral medication with high bioavailability. To assess the drug-likeness and oral bioavailability of the developed compounds, we used five rules: Lipinski (Lipinski et al., 2001), Ghose (Ghose et al., 1998), Veber (Veber et al., 2002), Egan (Egan and Lauri, 2002), and Muegge (Muegge et al., 2001). All the molecules have followed the five principles with few exceptions. Table 7 lists the features of compounds **8a**–**j** that relate to drug similarity. The bioavailability scores of all the compounds studied were found to be 0.55 except for acarbose (0.17), indicating good compliance. The pan assay interference compounds (PAINS) warnings are zero, indicating that the lead molecules' pharmacokinetic profile is favorable. When compared to the reference drug, acarbose, the majority of the compounds showed good physicochemical, pharmacokinetic, and drug likeliness features.

2.2.2 *In silico* molecular docking study

All the designed molecules were screened further *in silico* for their ability to bind with pancreatic α-amylase enzyme using 1-click docking online server tool (http://mcule.com/apps/1-click-docking/) authorized by AutoDock Vina docking algorithm (Trott and Olson, 2010). The screening results depicted that all molecules showed better or nearly

Table 6: Pharmacokinetic/ADME properties of compounds **8a–j**

Compound	[a]GI absorption	[b]BBB permeant	[c]Pgp substrate	[d]CYP1A2 inhibitor	[e]CYP2C19 inhibitor	[f]CYP2C9 inhibitor	[g]CYP2D6 inhibitor	[h]CYP3A4 inhibitor	[i]log *Kp* ($cm \cdot s^{-1}$)
8a	Low	No	Yes	No	Yes	Yes	Yes	Yes	−7.08
8b	Low	No	No	No	Yes	Yes	No	Yes	−6.04
8c	Low	No	No	No	Yes	Yes	No	Yes	−6.46
8d	Low	No	No	No	Yes	Yes	No	Yes	−6.27
8e	Low	No	No	No	Yes	Yes	Yes	Yes	−6.61
8f	Low	No	No	Yes	Yes	Yes	No	Yes	−6.33
8g	Low	No	Yes	No	Yes	Yes	No	Yes	−6.49
8h	Low	No	No	No	Yes	Yes	No	Yes	−7
8i	Low	No	No	No	Yes	Yes	No	Yes	−7.05
8j	Low	No	No	No	Yes	Yes	No	Yes	−6.84
Acarbose	Low	No	Yes	No	No	No	No	No	−16.29

[a]Gastrointestinal absorption; [b]blood–brain barrier permeant; [c]p-glycoprotein substrate; [d]CYP1A2: Cytochrome P450 family 1 subfamily A member 2; [e]CYP2C19: Cytochrome P450 family 2 subfamily C member 19; [f]CYP2C9: Cytochrome P450 family 2 subfamily C member 9; [g]CYP2D6: Cytochrome P450 family 2 subfamily D member 6; [h]CYP3A4: Cytochrome P450 family 3 subfamily A member 4; [i]skin permeation in $cm \cdot s^{-1}$.

Table 7: Drug likeness properties of compounds **8a–j**

Compound	Lipinski violations	Ghose violations	Veber violations	Egan violations	Muegge violations	Bioavailability score	PAINS alerts	Synthetic accessibility
8a	0	0	1	1	0	0.55	0	4.53
8b	1	2	1	1	0	0.55	0	4.73
8c	0	2	1	1	0	0.55	0	4.75
8d	0	2	1	1	0	0.55	0	4.81
8e	0	2	0	1	0	0.55	0	4.78
8f	1	2	1	1	1	0.55	0	4.69
8g	0	2	1	1	0	0.55	0	4.73
8h	1	2	1	1	1	0.55	0	5.04
8i	1	2	1	1	1	0.55	0	4.99
8j	1	2	1	1	1	0.55	0	5.16
Acarbose	3	4	1	1	5	0.17	0	7.34

equal binding energies (−8.6 to −7.6 $kcal \cdot mol^{-1}$) on comparison with reference drug, acarbose (−8.2 $kcal \cdot mol^{-1}$). The comprehensive data of binding energies and the corresponding bonding pose of complexes are shown in Table S1.

All the screened molecules (**8a**–**j**) have shown good docking with binding energies in the range −7.9 to 8.6 $kcal \cdot mol^{-1}$. Among the 10 molecules in this series, the molecules **8b**, **8d**, **8f**, **8i**, and **8j** have shown equal or greater binding energies when compared with reference drug (Table S1). In compound **8b**, the iso-quinoline formed π–π stacking with His305. In addition, the molecule formed hydrophobic interactions with residues such as Leu237, Ile235, Trp58, Trp59, Ala198, Tyr 62, Leu165, Leu162, Ala307, and Tyr151. In molecule **8d**, oxygen atom of thiazolidine-dione formed hydrogen bonding with Lys200. Additionally, the molecule also formed hydrophobic contacts with residues Tyr151, Ala198, Ile235, Trp58, Trp59, Tyr62, Leu165, and Leu162. In molecule **8f**, the oxygen atom of thiazolidine-dione formed hydrogen bonding with Gln63. Additionally, the phenyl and benzothiazole rings have formed π–π stacking with the residues His305 and His201, respectively. The hydrophobic interactions are formed by this molecule with Tyr62, Tyr151, Trp59, Trp58, Ile235, Val234, Ala198, Leu162, and Leu165. In molecule **8i**, oxygen atom of both chromone and thiazolidine-dione rings formed hydrogen bonding with His305 and Lys200, respectively. The molecule **8i** also formed hydrophobic contacts with residues, namely, Tyr151, Ile235, Ala198, Trp58, Trp59, Tyr62, Leu165, and Leu162. The molecule **8j** showed the best binding energy among the screened molecules. Hydrogen

bonding is formed by both oxygen atoms of thiazolidine-dione ring with residues, namely, Lys200 and Tyr151. It is observed that, π–π stacking is formed between chromone ring and Trp59. Besides, this molecule also formed hydrophobic contacts with Leu165, Leu162, Ala198, Tyr62, Trp59, Trp58, Tyr151, and Ile235. In scientific literature, 2D diagrams are used to recognize the binding interactions of the target protein with the ligands. These 2D ligand diagrams of the molecules **8b, 8d**, **8f**, **8i**, and **8j** which depict their binding contacts with target enzyme are given in Table 8.

2.2.3 α-Amylase inhibitory activity

The synthesized compounds were screened *in vitro* for their ability to inhibit α-Amylase using a standard method (Nickavar and Amin, 2011; Patil et al., 2013) with slight amendments. The screening was carried out at concentrations of 25, 50, 100, 150, and 200 μg·mL^{-1}. Majority of the compounds showed good inhibition towards the target enzyme. The compound **8j** bearing with 6-methyl-4-oxo-4*H*-chromen-3-yl moiety has shown the highest inhibitory activity amongst the screened compounds with IC_{50} value of 100.5 ± 0.2 μg·mL^{-1}. The compound **8d** bearing benzofuran-2-yl substituent has shown the second highest inhibition with IC_{50} value of 108.6 ± 0.2 μg·mL^{-1}. The **8g** having 1*H*-indol-5-yl substituent has shown the third highest inhibition with IC_{50} value of 110.9 ± 0.3 μg·mL^{-1}. The compounds **8h** bearing *6-bromo-4-oxo-4H-chromen-3-yl* moiety and **8f** with benzothiazol-2-yl substituent have shown the inhibition next to these compounds with IC_{50} values of 115.0 ± 0.1 and 118.9 ± 0.2 μg·mL^{-1}, respectively. The remaining compounds **8a**, **8b**, **8c**, **8e**, and **8i** exhibited moderate inhibition on the enzyme with IC_{50} ranging

Table 8: 2D LIGPLOT images of compounds **8b, 8d, 8e, 8i**, and **8j**

Compound	2D structure	Compound	2D structure
8b	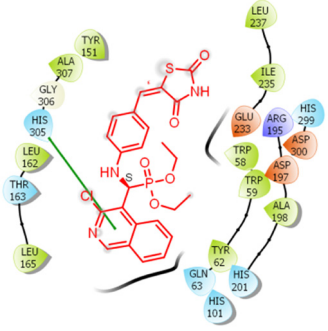	**8i**	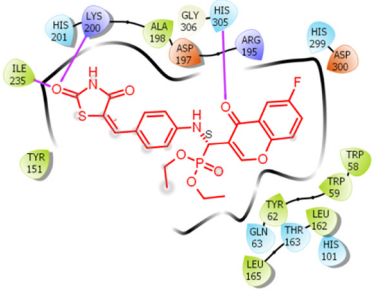
8d	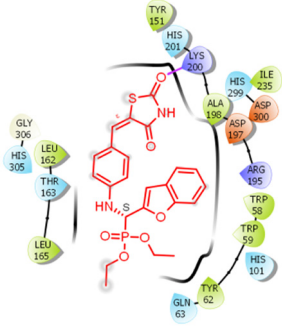	**8j**	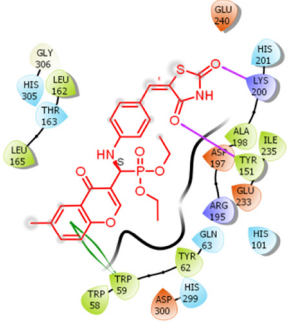
8f	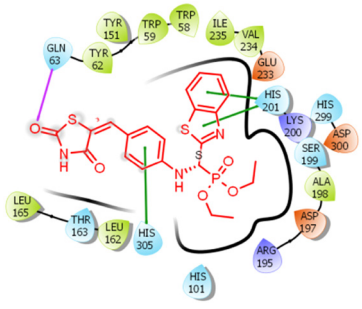		

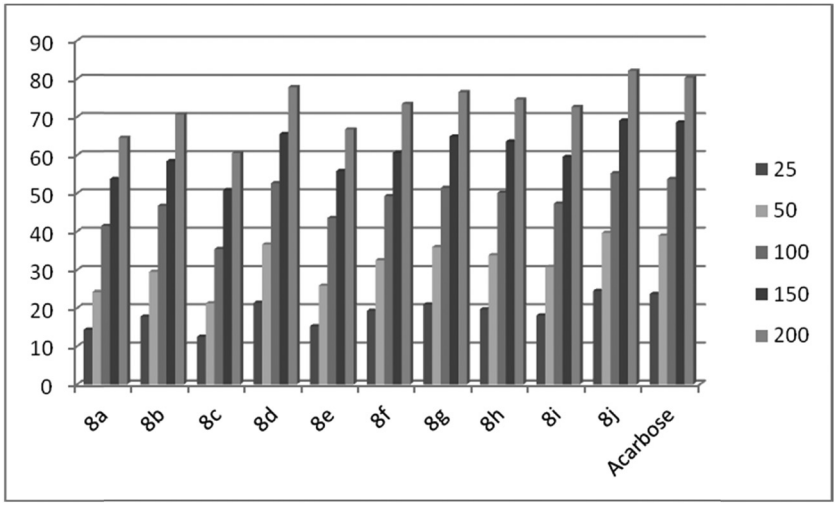

Figure 1: α-Amylase inhibition activity results of compounds **8a–j**.

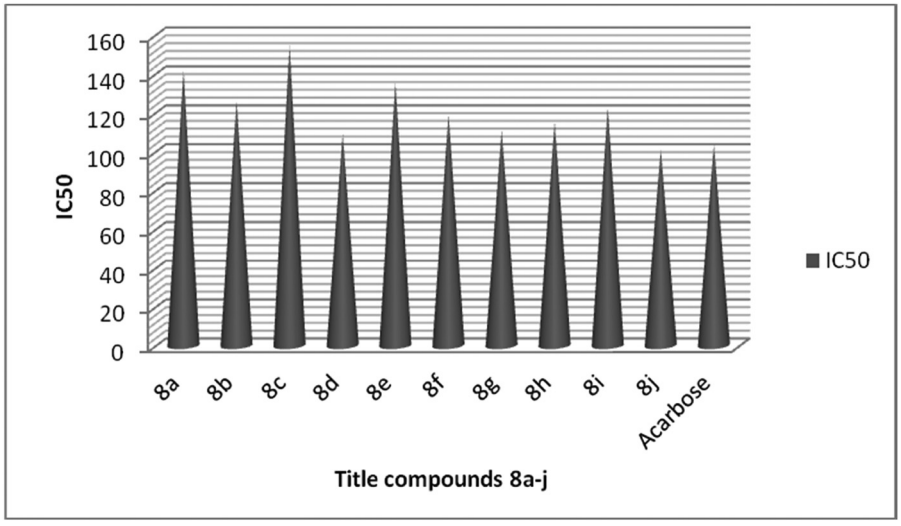

Figure 2: IC_{50} values of compounds **8a–j**.

from 122.3 ± 0.3 to 154.3 ± 0.6 μg·mL^{-1}. The results pertaining to % inhibition and IC_{50} values of all the compounds **8a–j** are presented in Figures 1 and 2, respectively.

3 Conclusion

A greener approach was developed for the synthesis of new α-Aps **8a–j** *via* one pot K–F reaction in high yields under solvent free condition using nano Sb_2O_3 as reusable catalyst. Prior to synthesis, compounds were designed to mimic ADMET and molecular docking in order to identify the most promising candidates for subsequent drug development. Molecules **8a–j**, which are predicted based on the five principles and have strong oral bioavailability, are identified in a library of tested molecules with drug-likeness and good oral bioavailability. All compounds are poorly absorbed through the GI tract and do not permeate the BBB, hence they are not a Pgp substrate. When compared to the reference drug, the PAINS warnings are zero, indicating that the lead compounds have an outstanding pharmacokinetic profile. The results of the molecular docking analysis revealed that all of the compounds examined showed effective inhibition of the target enzyme. The synthesis of compounds with good drug-like behavior and the ability to block the target enzyme, α-amylase, was prompted. This cut down on drug development time, expense, and chemical waste. The spectrophotometric technique was

used to test *in vitro* α-amylase inhibitory activity for all the newly synthesized compounds. The compound **8j** showed superior inhibition against the target enzyme than reference drug. The compounds **8d**, **8g**, **8h,** and **8f** exhibited close inhibitory activity in comparison with a standard. When compared to the conventional drug, acarbose, most of the compounds showed considerable inhibition of the target enzyme. The results of this study show that the synthesized compounds will be promising next-generation anti-diabetic medications that can be utilized to successfully treat symptoms of diabetes complications.

Experimental methods

Materials and characterization techniques

Using MarvinView software, the structures of all the compounds were sketched, optimized, and transferred into the appropriate format. The 1-Click docking software, which is driven by the AutoDock Vina docking algorithm, was used to conduct the *in silico* molecular docking study. The structures of all the compounds were drawn, optimized, and converted into the required format using MarvinView software. *In silico* molecular docking study was done using 1-Click docking software powered by AutoDock Vina docking algorithm. To calculate IC_{50} values and to draw the graphs related to the biological activity, GraphPad Prism 9 software was used. The chemicals were purchased from SD Fine Chem. Ltd, India, and only a small percentage of them were refined using normal methods. All the reactions took place on a magnetic agitator that also served as a hot plate. The purity of the compounds was checked by thin-layer chromatography (TLC) on an Al sheet of silica gel. NMR spectra of ^{31}P (161.9 MHz), ^{1}H (400 MHz), and ^{13}C (100 MHz) were recorded using a Bruker AMX spectrometer. On the SHIMADZU 2010A, Liquid chromatography–mass spectrometry (LCMS) was recorded and CHN analysis was performed on the T. F. Flash 1112 apparatus. The IR spectra were documented using a Fourier transform infrared spectrometer (Bruker IFS 55, Equinox) in KBr. Chemical shift, coupling constants, and *J* values were all expressed in Hz and ppm, respectively. Peaks in NMR spectra were represented by the symbol "s" for singlet, "d" for doublet, "t" for triplet, and "m" for multiplet. Single-mode MW synthesis apparatus was used for MW irradiation experiments.

Procedure

Synthesis of 2,4-thiazolidinedione (3)

In a reaction vessel, a solution of chloroacetic acid (1) (4.73 g, 0.05 mol) in water (20 mL) and thiourea (2) (3.81 g, 0.05 mol) in water (20 mL) were mixed and agitated for 15 min to produce a white ppt on cooling. 5 mL of concentrated HCl was gently added using a dropping funnel, and the mixture was refluxed for 10–15 h at roughly 105°C. A cluster of white needle-shaped compound was obtained after cooling. HCl traces were eliminated by washing with water and drying. Finally, the pure compound (**3**) was obtained by recrystallizing from ethyl alcohol, with a melting point of 122–124°C (Prashantha Kumar et al., 2011).

Synthesis of (*E*)-5-(4-aminobenzylidene)thiazolidine-2,4-dione (5)

In the presence of a catalytic quantity of piperidine, *p*-amino benzaldehyde (4.85 g, 0.04 mol) (**4**) was added to 2,4-thiazolidinedione (**3**) (5.85 g, 0.05 mol) in toluene (20 mL) and refluxed at 110°C for roughly 6 h before cooling to room temperature to precipitate off the (*E*)-5-(4-aminobenzylidene)thiazolidine-2,4-dione (**5**). To check the progress of the process, TLC (eluent: ethyl acetate: *n*-hexane, 5:5) was utilized. (**5**): Solid; yield, 93%; melting point (MP): 187–189°C; δ_H (DMSO-d_6): 12.23 (s, 1H, NH), 7.13 (s, 1H, = C–H), 7.09 (d, 2H, J = 7.6 Hz, Ar–H), 6.58 (d, 2H, J = 7.6 Hz, Ar–H), 3.86 (br-s, 2H, NH_2); δ_C (DMSO-d_6): 165.5 (C-1), 164.3 (C-3), 113.5 (C-5), 143.5 (C-6), 123.2 (C-7), 126.4 (C-8, C-12), 115.4 (C-9, C-11), 149.6 (C-10) (Kawade et al., 2017; Sujatha et al., 2020; Young et al., 2012).

MW-assisted synthesis of α-Aps (8a–j)

The mixture of picolinaldehyde (**6a**) (2.14 g, 0.020 mol), diethyl (4-(2,4-dichlorophenyl)thiazol-2-ylamino)(phenyl) methyl-phosphonate (**5**) (4.40 g, 0.020 mol), diethyl phosphite (**7**) (2.6 mL, 0.020 mol) were placed in a flat bottomed flask. To this mixture, nano Sb_2O_3 (10 mol%) was added and the mixture was MW irradiated at 450 W under solvent free condition at ambient temperature for about 15 min. The progress of the reaction was monitored by TLC (ethyl-acetate: *n*-hexane, 4:6). After completion of the reaction as checked by TLC, the reaction mixture was cooled to room temperature. DCM (15 mL) was added to the reaction content and stirred for 10 min. The catalyst, nano Sb_2O_3 was

separated by filtration as residue, washed with DCM (2 mL × 10 mL) and the residue was dried under vacuum at 100°C to utilize in further studies. The combined organic layer was washed with water (15 mL), dried over anhydrous Na_2SO_4, and concentrated under vacuum at 50°C to obtain the crude product. The pure compound, diethyl (4-((*E*)-(2,4-dioxothiazolidin-5-ylidene)methyl)phenylamino)(pyridin-2-yl)methylphosphonate (**8a**) was obtained by column chromatography using ethyl acetate: *n*-hexane (7:3) as eluent. The same procedure was used for the preparation of the remaining compounds **8b–j.**

Characterization of title compounds 8a–j

The general structure of title compunds (**8a–j**) is presented in Figure 3.

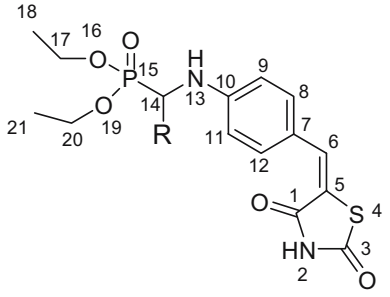

Figure 3: General structure of title compounds **8a–j**.

Diethyl (4-((*E*)-(2,4-dioxothiazolidin-5-ylidene)methyl) phenylamino)(pyridin-2-yl)methylphosphonate (8a)

Yield: 89%; solid, MP 176–178°C; δ_H (DMSO-d_6): 11.52 (s, 1H, –NH), 8.52 (d, J = 7.2 Hz, 1H, Py-H), 7.74 (t, J = 7.6 Hz, 1H, Py-H), 7.48 (d, J = 7.2 Hz, 1H, Py-H), 7.21 (t, J = 8.0 Hz, 1H, Py-H), 7.12 (s, 1H, =CH), 7.02 (d, J = 7.2 Hz, 2H, Ar-H), 6.33 (d, J = 7.6 Hz, 2H, Ar–H), 5.71 (d, 1H, N–H), 4.19 (q, 4H, O–$\underline{CH_2}\underline{CH_3}$), 3.90 (d, 1H, P–CH–), 1.21 (t, J = 6.8 Hz, 6H, O–$CH_2\underline{CH_3}$); δ_C (DMSO-d_6): 164.5 (C-1), 165.8 (C-3), 116.3 (C-5), 141.3 (C-6), 122.4 (C-7), 128.1 (C-8 and C-12), 112.7 (C-9 and C-11), 145.9 (C-10), 54.6 (C-14), 63.5 (C-17 and C-20), 13.7 (C-18 and C-21), 157.4 (C-22), 147.8 (C-17), 120.7 (C-25), 137.4 (C-26), 125.7 (C-27); δ_P (DMSO-d_6): 15.7 ppm; IR (KBr) (ν_{max} cm^{-1}): 3,330, 3,125 (NH), 1,206 (P=O), 1,017 (P–O–C_{alip}); LCMS (m/z, %): 448 ($M + H^+$, 100); For $C_{20}H_{22}N_3O_5PS$, calculated: C, 53.69%; H, 4.96%; N, 9.39%; found: C, 53.80%; H, 4.83%; N, 9.52%.

Diethyl (4-((*E*)-(2,4-dioxothiazolidin-5-ylidene)methyl) phenylamino)(3-chloroisoquinolin-4-yl) methylphosphonate (8b)

Yield: 91%; solid, MP 182–184°C; δ_H (DMSO-d_6): 11.52 (s, 1H, –NH), 9.10 (s, 1H, isoqui-H), 7.89 (d, 1H, isoqui-H), 7.80 (d, 1H, isoqui-H), 7.51 (t, 1H, isoqui-H), 7.42 (t, 1H, isoqui-H), 7.12 (s, 1H, =CH), 7.02 (d, J = 7.2 Hz, 2H, Ar–H), 6.33 (d, J = 7.6 Hz, 2H, Ar–H), 5.71 (d, 1H, N–H), 4.19 (q, 4H, O–$\underline{CH_2}\underline{CH_3}$), 3.90 (d, 1H, P–CH–), 1.21 (t, J = 6.8 Hz, 6H, O–$CH_2\underline{CH_3}$); δ_C (DMSO-d_6): 164.5 (C-1), 165.8 (C-3), 116.3 (C-5), 141.3 (C-6), 122.4 (C-7), 128.1 (C-8 and C-12), 112.7 (C-9 and C-11), 145.9 (C-10), 54.6 (C-14), 63.5 (C-17 and C-20), 13.7 (C-18 and C-21), 125.3 (C-22), 133.4 (C-23), 127.5 (C-24), 151.3 (C-25), 149.2 (C-27), 120.5 (C-28), 129.8 (C-29), 125.6 (C-30), 127.8 (C-31); δ_P (DMSO-d_6): 19.4 ppm; IR (KBr) (ν_{max} cm^{-1}): 3,295, 3,147 (NH), 1,210 (P=O), 1,004 (P–O–C_{alip}); LCMS (m/z, %): 532 ($M + H^+$, 100); For $C_{24}H_{23}ClN_3O_5PS$, calculated: C, 54.19%; H, 4.36%; N, 7.90%; found: C, 54.07%; H, 4.49%; N, 7.75%.

Diethyl (4-((*E*)-(2,4-dioxothiazolidin-5-ylidene)methyl) phenylamino)(quinolin-4-yl)methylphosphonate (8c)

Yield: 90%; solid, MP 191–193°C; δ_H (DMSO-d_6): 11.52 (s, 1H, –NH), 8.51 (d, 1H, Qui-H), 8.07 (d, 1H, Qui-H), 7.82 (d, 1H, Qui-H), 7.51 (t, 1H, Qui-H), 7.38 (t, 1H, Qui-H), 7.08 (d, 1H, Qui-H), 7.12 (s, 1H, =CH), 7.02 (d, J = 7.2 Hz, 2H, Ar–H), 6.33 (d, J = 7.6 Hz, 2H, Ar–H), 5.71 (d, 1H, N–H), 4.19 (q, 4H, O–$\underline{CH_2}\underline{CH_3}$), 3.90 (d, 1H, P–CH–), 1.21 (t, J = 6.8 Hz, 6H, O–$CH_2\underline{CH_3}$); δ_C (DMSO-d_6): 164.5 (C-1), 165.8 (C-3), 116.3 (C-5), 141.3 (C-6), 122.4 (C-7), 128.1 (C-8 and C-12), 112.7 (C-9 and C-11), 145.9 (C-10), 54.6 (C-14), 63.5 (C-17 and C-20), 13.7 (C-18 and C-21), 140.3 (C-22), 126.6 (C-23), 147.3 (C-24), 151.5 (C-26), 123.2 (C-27), 123.5 (C-28), 127.4 (C-29), 128.8 (C-30), 128.6 (C-31); δ_P (DMSO-d_6): 18.2 ppm; IR (KBr) (ν_{max} cm^{-1}): 3,331, 3,136 (NH), 1,215 (P=O), 1,008 (P–O–C_{alip}); LCMS (m/z, %): 498 ($M + H^+$, 100); For $C_{24}H_{24}N_3O_5PS$, calculated: C, 57.94%; H, 4.86%; N, 8.45%; found: C, 57.82%; H, 4.99%; N, 8.31%.

Diethyl (4-((*E*)-(2,4-dioxothiazolidin-5-ylidene)methyl) phenylamino)(benzofuran-2-yl)methylphosphonate (8d)

Yield: 94%; solid, MP 231–233°C; δ_H (DMSO-d_6): 11.52 (s, 1H, –NH), 7.42 (d, 1H, benzofuran-H), 7.37 (d, 1H,

benzofuran-H), 7.23 (t, 1H, benzofuran-H), 7.14 (t, 1H, benzofuran-H), 7.12 (s, 1H, =CH), 7.02 (d, J = 7.2 Hz, 2H, Ar–H), 6.53 (t, 1H, benzofuran-H), 6.33 (d, J = 7.6 Hz, 2H, Ar–H), 5.71 (d, 1H, N–H), 4.19 (q, 4H, O–$\underline{CH_2}CH_3$), 3.90 (d, 1H, P–CH–), 1.21 (t, J = 6.8 Hz, 6H, O–$CH_2\underline{CH_3}$); δ_C (DMSO-d_6): 164.5 (C-1), 165.8 (C-3), 116.3 (C-5), 141.3 (C-6), 122.4 (C-7), 128.1 (C-8 and C-12), 112.7 (C-9 and C-11), 145.9 (C-10), 54.6 (C-14), 63.5 (C-17 and C-20), 13.7 (C-18 and C-21), 153.3 (C-22), 104.5 (C-23), 127.8 (C-24), 153.7 (C-25), 122.4 (C-27), 123.2 (C-28), 125.6 (C-29), 118.2 (C-30); δ_P (DMSO-d_6): 21.4 ppm; IR (KBr) (ν_{max} cm^{-1}): 3,324, 3,188 (NH), 1,220 (P=O), 1,012 (P–O–C_{alip}); LCMS (m/z, %): 487 ($M + H^+$, 100); For $C_{23}H_{23}N_2O_6PS$, calculated: C, 56.78%; H, 4.77%; N, 5.76%; found: C, 56.91%; H, 4.64%; N, 5.89%.

Diethyl (4-((*E*)-(2,4-dioxothiazolidin-5-ylidene)methyl) phenylamino)(1-methyl-1H-indol-3-yl) methylphosphonate (8e)

Yield: 92%; solid, MP 204–206°C; δ_H (DMSO-d_6): 11.52 (s, 1H, –NH), 7.37 (s, 1H, indole-H), 7.29 (t, J = 7.2 Hz, 1H, indole-H), 7.21 (t, J = 7.2 Hz, 1H, indole-H), 7.12 (s, 1H, =CH), 7.02 (d, J = 7.2 Hz, 2H, Ar–H), 6.89 (d, J = 7.2 Hz, 1H, indole-H), 6.78 (d, J = 7.2 Hz, 1H, indole-H), 6.33 (d, J = 7.6 Hz, 2H, Ar–H), 5.71 (d, 1H, N–H), 4.19 (q, 4H, O–$\underline{CH_2}CH_3$), 3.90 (d, 1H, P–CH–), 3.45 (s, 3H, –CH_3), 1.21 (t, J = 6.8 Hz, 6H, O–$CH_2\underline{CH_3}$); δ_C (DMSO-d_6): 164.5 (C-1), 165.8 (C-3), 116.3 (C-5), 141.3 (C-6), 122.4 (C-7), 128.1 (C-8 and C-12), 112.7 (C-9 and C-11), 145.9 (C-10), 54.6 (C-14), 63.5 (C-17 and C-20), 13.7 (C-18, C-21), 113.2 (C-22), 126.5 (C-23), 137.9 (C-24), 125.8 (C-26), 118.4 (C-27), 123.4 (C-28), 120.4 (C-29), 110.5 (C-30), 43.4 (C-31); δ_P (DMSO-d_6): 17.9 ppm; IR (KBr) (ν_{max} cm^{-1}): 3,315, 3,145 (NH), 1,217 (P=O), 1,005 (P–O–C_{alip}); LCMS (m/z, %): 500 ($M + H^+$, 100); For $C_{24}H_{26}N_3O_5PS$, Calculated: C, 57.71%; H, 5.25%; N, 8.41%; found: C, 57.58%; H, 5.37%; N, 8.28%.

Diethyl (4-((*E*)-(2,4-dioxothiazolidin-5-ylidene)methyl) phenylamino)(benzo[d]thiazol-2-yl) methylphosphonate (8f)

Yield: 90%; solid, MP 213–215°C; δ_H (DMSO-d_6): 11.52 (s, 1H, –NH), 7.12 (s, 1H, =CH), 8.17 (d, J = 7.2 Hz, 1H, Ar–H), 8.06 (d, J = 7.2 Hz, 1H, Ar–H), 7.43 (t, J = 7.2 Hz, 2H, Ar–H), 6.33 (d, J = 7.6 Hz, 2H, Ar–H), 5.71 (d, 1H, N–H), 4.19 (q, 4H, O–$\underline{CH_2}CH_3$), 3.90 (d, 1H, P–CH–), 1.21 (t, J = 6.8 Hz, 6H, O–$CH_2\underline{CH_3}$); δ_C (DMSO-d_6): 164.5 (C-1), 165.8 (C-3), 116.3 (C-5), 141.3 (C-6), 122.4 (C-7), 128.1 (C-8 and C-12), 112.7 (C-9 and C-11), 145.9 (C-10), 54.6 (C-14), 63.5 (C-17 and C-20), 13.7 (C-18 and C-21), 167.3 (C-22), 151.8 (C-24), 135.1 (C-25), 120.4 (C-27), 126.7 (C-28), 127.3 (C-29), 121.2 (C-30); δ_P (DMSO-d_6): 25.3 ppm; IR (KBr) (ν_{max} cm^{-1}): 3,311, 3,166 (NH), 1,215 (P=O), 1,010 (P–O–C_{alip}); LCMS (m/z, %): 504 ($M + H^+$, 100); For $C_{22}H_{22}N_3O_5PS_2$, calculated: C, 52.48%; H, 4.40%; N, 8.35%; found: C, 52.60%; H, 4.29%; N, 8.47%.

Diethyl (4-((*E*)-(2,4-dioxothiazolidin-5-ylidene)methyl) phenylamino)(1H-indol-5-yl)methylphosphonate (8g)

Yield: 93%; solid, MP 166–168°C; δ_H (DMSO-d_6): 11.52 (s, 1H, –NH), 7.32 (d, J = 7.2 Hz, 1H, indole-H), 7.26 (d, J = 7.2 Hz, 1H, indole-H), 7.17 (d, J = 7.2 Hz, 1H, indole-H), 7.12 (s, 1H, =CH), 7.02 (d, J = 7.2 Hz, 2H, Ar–H), 6.76 (d, J = 7.2 Hz, 1H, indole-H), 6.33 (d, J = 7.6 Hz, 2H, Ar–H), 6.25 (d, J = 7.2 Hz, 1H, indole-H), 5.71 (d, 1H, N–H), 4.19 (q, 4H, O–$\underline{CH_2}CH_3$), 3.90 (d, 1H, P–CH–), 1.21 (t, J = 6.8 Hz, 6H, O–$CH_2\underline{CH_3}$); δ_C (DMSO-d_6): 164.5 (C-1), 165.8 (C-3), 116.3 (C-5), 141.3 (C-6), 122.4 (C-7), 128.1 (C-8 and C-12), 112.7 (C-9 and C-11), 145.9 (C-10), 54.6 (C-14), 63.5 (C-17 and C-20), 13.7 (C-18, C-21), 134.1 (C-22), 117.3 (C-23), 128.4 (C-24), 132.6 (C-25), 109.8 (C-26), 117.3 (C-27), 101.2 (C-28), 123.5 (C-29); δ_P (DMSO-d_6): 22.6 ppm; IR (KBr) (ν_{max} cm^{-1}): 3,372, 3,292, 3,177 (NH), 1,218 (P=O), 1,011 (P–O–C_{alip}); LCMS (m/z, %): 486 ($M + H^+$, 100); For $C_{23}H_{24}N_3O_5PS$, calculated: C, 56.90%; H, 4.98%; N, 8.66%; found: C, 56.99%; H, 4.82%; N, 8.78%.

Diethyl (4-((*E*)-(2,4-dioxothiazolidin-5-ylidene)methyl) phenylamino)(6-bromo-4-oxo-4H-chromen-3-yl) methylphosphonate (8h)

Yield: 89%; solid, MP 158–160°C; δ_H (DMSO-d_6): 11.52 (s, 1H, –NH), 7.75 (s, 1H, Ar–H), 7.42 (d, J = 7.2 Hz, 1H, Ar–H), 7.15 (s, 1H, = C–H), 6.78 (d, J = 7.2 Hz, 1H, Ar–H), 7.12 (s, 1H, =CH), 7.02 (d, J = 7.2 Hz, 2H, Ar–H), 6.33 (d, J = 7.6 Hz, 2H, Ar–H), 5.71 (d, 1H, N–H), 4.19 (q, 4H, O–$\underline{CH_2}CH_3$), 3.90 (d, 1H, P–CH–), 1.21 (t, J = 6.8 Hz, 6H, O–$CH_2\underline{CH_3}$); δ_C (DMSO-d_6): 164.5 (C-1), 165.8 (C-3), 116.3 (C-5), 141.3 (C-6), 122.4 (C-7), 128.1 (C-8 and C-12), 112.7 (C-9 and C-11), 145.9 (C-10), 54.6 (C-14), 63.5 (C-17 and C-20), 13.7 (C-18 and C-21), 117.5 (C-22), 152.3 (C-23), 157.5 (C-25), 127.9 (C-26), 181.8 (C-27), 118.3 (C-28), 139.7 (C-29), 116.4 (C-30), 135.8 (C-31); δ_P (DMSO-d_6): 18.7 ppm; IR (KBr) (ν_{max} cm^{-1}): 3,311, 3,159 (NH), 1,213 (P=O), 1,007 (P–O–C_{alip}); LCMS (m/z, %): 593 ($M + H^+$, 100); For $C_{24}H_{22}BrN_2O_7PS$, calculated: C, 48.58%; H, 3.74%; N, 4.72%; found: C, 48.70%; H, 3.60%; N, 4.85%.

Diethyl (4-((*E*)-(2,4-dioxothiazolidin-5-ylidene)methyl) phenylamino)(6-fluoro-4-oxo-4H-chromen-3-yl) methylphosphonate (8i)

Yield: 95%; solid, MP 224–226°C; δ_H (DMSO-d_6): 11.52 (s, 1H, –NH), 7.45 (s, 1H, Ar–H), 7.12 (s, 1H, =CH), 7.18 (s, 1H, = C–H), 7.03 (d, J = 7.2 Hz, 1H, Ar–H), 6.72 (d, J = 7.2 Hz, 1H, Ar–H), 7.02 (d, J = 7.2 Hz, 2H, Ar–H), 6.33 (d, J = 7.6 Hz, 2H, Ar–H), 5.71 (d, 1H, N–H), 4.19 (q, 4H, O–$\underline{CH_2}\underline{CH_3}$), 3.90 (d, 1H, P–CH–), 1.21 (t, J = 6.8 Hz, 6H, O–$CH_2\underline{CH_3}$); δ_C (DMSO-d_6): 164.5 (C-1), 165.8 (C-3), 116.3 (C-5), 141.3 (C-6), 122.4 (C-7), 128.1 (C-8 and C-12), 112.7 (C-9, C-11), 145.9 (C-10), 54.6 (C-14), 63.5 (C-17 and C-20), 13.7 (C-18 and C-21), 117.5 (C-22), 152.3 (C-23), 157.5 (C-25), 127.9 (C-26), 181.8 (d, J = 242 Hz, C-27), 118.7 (C-28), 123.7 (C-29), 156.4 (C-30), 114.9 (C-31); δ_P (DMSO-d_6): 20.9 ppm; IR (KBr) (ν_{max} cm^{-1}): 3,345, 3,192 (NH), 1,221 (P=O), 1,012 (P–O–C_{alip}); LCMS (m/z, %): 533 (M + H^+, 100); For $C_{24}H_{22}FN_2O_7PS$, calculated: C, 54.13%; H, 4.16%; N, 5.26%; found: C, 54.25%; H, 4.04%; N, 5.39%.

Diethyl (4-((*E*)-(2,4-dioxothiazolidin-5-ylidene)methyl) phenylamino)(6-methyl-4-oxo-4H-chromen-3-yl) methylphosphonate (8j)

Yield: 94%; solid, MP 238–240°C; δ_H (DMSO-d_6): 11.52 (s, 1H, –NH), 7.41 (s, 1H, Ar–H), 7.13 (d, J = 7.2 Hz, 1H, Ar–H), 7.18 (s, 1H, = C–H), 7.12 (s, =CH), 7.02 (d, J = 7.2 Hz, 2H, Ar–H), 6.73 (d, J = 7.2 Hz, 1H, Ar–H), 2.26 (s, 3H, CH_3), 6.33 (d, J = 7.6 Hz, 2H, Ar–H), 5.71 (d, 1H, N–H), 4.19 (q, 4H, O–$\underline{CH_2}\underline{CH_3}$), 3.90 (d, 1H, P–CH–), 1.21 (t, J = 6.8 Hz, 6H, O–$CH_2\underline{CH_3}$); δ_C (DMSO-d_6): 164.5 (C-1), 165.8 (C-3), 116.3 (C-5), 141.3 (C-6), 122.4 (C-7), 128.1 (C-8 and C-12), 112.7 (C-9 and, C-11), 145.9 (C-10), 54.6 (C-14), 63.5 (C-17 and C-20), 13.7 (C-18 and C-21), 117.5 (C-22), 152.3 (C-23), 157.2 (C-25), 123.9 (C-26), 181.8 (C-27), 118.3 (C-28), 138.6 (C-29), 132.6 (C-30), 131.3 (C-31), 25.5 (C-32); δ_P (DMSO-d_6): 16.8 ppm; IR (KBr) (ν_{max} cm^{-1}): 3,305, 3,145 (NH), 1,210 (P=O), 1,005 (P–O–C_{alip});LCMS (m/z, %): 529 (M + H^+, 100); For $C_{25}H_{25}N_2O_7PS$, calculated: C, 56.81%; H, 4.77%; N, 5.30%; found: C, 56.69%; H, 4.89%; N, 5.17%.

In silico analysis

Using the Swiss ADME tool from the Swiss Institute of Bioinformatics (http://www.sib.swiss), all the designed molecules were *in silico* predicted for their physicochemical, lipophilicity, water-solubility, pharmacokinetic/ADME, drug-likeness properties, and medicinal chemistry.

In silico molecular docking studies

The binding mechanism of **8a**–**j** with the targeted enzyme, pancreatic α-amylase, was investigated using *in silico* molecular docking. The RCSB, Protein Data Bank, was used to obtain the crystal structure of this enzyme (PDB ID: 3IJ8). Water molecules, heteroatoms, and co-factors were removed from the structure to make it more efficient. Charges, hydrogen bonds, and atoms that were missing were added. The process of docking ligands with proteins and their interactions were investigated using the discovery studio visualizer V16.1.0.15350 (Madhu Kumar Reddy et al., 2019).

α-Amylase inhibitory activity

All the newly synthesized compounds were screened for their inhibitory activity against α-amylase using standard protocol through minor changes reported by Nickavar and Amin (2011) which was at first proposed by Patil et al. (2013) (see Supplementary material for detailed procedure).

One of the best measures of a drug's efficiency is IC_{50} (half-maximal inhibitory concentration). It reflects the amount of drug required to block a biological process by half, and so serves as a measure of antagonist drug potency in pharmacological research. In the present study, the IC_{50} values were calculated by plotting the concentration (X-axis) vs the percent inhibitory activity (Y-axis). Using the linear ($y = mx + c$) equation on this graph for y = 50 value x point becomes IC_{50} value. All the experiments were performed in triplicates and the results are expressed as mean value ± SD.

Acknowledgments: Authors acknowledge Dr. C. Naga Raju, Department of Chemistry, S. V. University, Tirupati for his constant support to complete this work.

Funding information: Authors state no funding involved.

Author contributions: Shaik Mohammad Altaff: conceptualization, resources, methodology, and investigation; Tiruveedula Raja Rajeswari: methodology and writing –

review and editing; Chennametty Subramanyam: validation, formal analysis, and writing – original draft.

Conflict of interest: Authors state no conflict of interest.

References

Allen M.C., Fuhrer W., Tuck B., Wade R., Wood J.M., Renin inhibitors. Synthesis of transition-state analog inhibitors containing phosphorus acid derivatives at the scissile bond. J. Med. Chem., 1989, 32, 1652–1661. doi: 10.1021/jm00127a041.

Altaff S.K.Md., Raja Rajeswari T., Subramanyam C., Synthesis, α-amylase inhibitory activity evaluation and *in silico* molecular docking study of some new phosphoramidates containing heterocyclic ring. Phosphorus Sulfur., 2021, 196(4), 389–397. doi: 10.1080/10426507.2020.1845679.

Angajala G., Subashini R., Sebastian M., Diabetes mellitus and human health care. Apple Academic Press, 2014, 229–246. doi: 10.1201/b16415-6.

Azaam M.M., Kenawy E.R., El-din S.B., Khamis A.A., El-Magd M.A., Antioxidant and anticancer activities of α-aminophosphonates containing thiadiazole moiety. J. Saudi. Chem. Soc., 2018, 22(1), 34–41. doi: 10.1016/j.jscs.2017.06.002.

Bagi P., Herbay R., Varga B., Fersch D., Fogassy E., Keglevich G., The preparation and application of optically active organophosphorus compounds. Phosphorus Sulfur., 2019, 194, 591–594. doi: 10.1080/10426507.2018.1547725.

Basha S.T., Sudhamani H., Rasheed S., Venkateswarlu N., Vijaya T., Raju C.N., Microwave-assisted neat synthesis of α-aminophosphonate/phosphinate derivatives of 2-(2-aminophenyl) benzothiazole as potent antimicrobial and antioxidant agents. Phosphorus Sulfur., 2016, 191, 1339–1343. doi: 10.1080/10426507.2016.1192629.

Bayer E., Gugel K., Hagen H., Jessipow S., Konig W., Zahner H., Metabolites of microorganisms. 98th communication. Phosphinothricin and phosphinothricyl-alanyl-alanine. Helv. Chim. Acta., 1972, 55, 224–239. doi: 10.1002/hlca.19720550744.

Bhattacharya A.K., Raut D.S., Rana K.C., Polanki I.K., Khan M.S., Iram S.E., Diversity-oriented synthesis of α-aminophosphonates: a new class of potential anticancer agents. J. Med. Chem., 2013, 66, 146–152. doi: 10.1016/j.ejmech.2013.05.036.

Bozdag-Dündar O., Verspohl E.J., Daş-Evcimen N., Kaup R.M., Bauer K., Sarikaya M., et al., Synthesis and biological activity of some new flavonyl-2,4-thiazolidinediones. Bioorg. Med. Chem., 2008, 16(14), 6747–6751. doi: 10.1016/j.bmc.2008.05.059.

Brebua M., Jakab E., Sakata Y., Effect of flame retardants and Sb_2O_3 synergist on the thermal decomposition of high-impact polystyrene and on its debromination by ammonia treatment, J. Anal. Appl. Pyrolysis, 2007, 79, 346–352. doi: 10.1016/j.jaap.2007.02.003.

Ceriello A., Thiazolidinediones as anti-inflammatory and anti-atherogenic agents. Diabetes Metab. Res. Rev., 2008, 24(1), 14–26. doi: 10.1002/dmrr.790.

Chang P.R., Yu J., Ma X., Fabrication and characterization of Sb_2O_3/carboxymethyl cellulose sodium and the properties of plasticized starch composite films. Macromol. Mater. Eng., 2009, 294, 762–767. doi: 10.1002/mame.200900138.

Daina A., Zoete V., A BOILED-Egg to predict gastrointestinal absorption and brain penetration of small molecules. Chem. Med. Chem., 2016, 11, 1117–1121. doi: 10.1002/cmdc.201600182.

Damiche R., Chafaa S., Synthesis of new bioactive aminophosphonates and study of their antioxidant, anti-inflammatory and antibacterial activities as well the assessment of their toxicological activity. J. Mol. Struct., 2017, 1130, 1009–1017. doi: 10.1016/j.molstruc.2016.10.054.

De la Hoz A., Draz Ortiz A., Moreno A., Microwaves in organic synthesis. Thermal and non-thermal microwave effects. Chem. Soc. Rev., 2005, 34, 164–178. doi: 10.1039/B411438H.

Dhawan B., Redmore D., Optically active 1-aminoalkylphosphonic acids. Phosphorus Sulfur., 1987, 32, 119–144. doi: 10.1080/03086648708074270.

Duh B., Effect of antimony catalyst on solid-state polycondensation of poly(ethylene terephthalate). Polymer, 2002, 43, 3147–3154. doi: 10.1016/S0032-3861(02)00138-6.

Dzimitrowicz D.J., Goodenough J.B., Wiseman P.J., A.C. proton conduction in hydrous oxides. Mater. Res. Bull., 1982, 17, 971–979. doi: 10.1016/0025-5408(82)90122-2.

Egan W.J., Lauri G., Prediction of intestinal permeability. Adv. Drug Del. Rev., 2002, 54, 273–289. doi: 10.1016/s0169-409x(02)00004-2.

Eun J.S., Kim K.S., Kim H.N., Park S.A., Ma T.Z., Lee K.A. et al., Synthesis of psoralen derivatives and their blocking effect of hKv1.5 channel. Arch. Pharm. Res., 2007, 30(2), 155–160. doi: 10.1007/BF02977688

Farahani N., Akbari J., Organocatalytic synthesis of α-aminophosphonates using o-benzenedisul fonimide as a recyclable bronsted acid catalyst. Lett. Org. Chem., 2017, 14(7), 483–487. doi: 10.2174/1570178614666170321123731.

Ghafuri H., Rashidizadeh, A., Zand H.R.E., Highly efficient solvent free synthesis of α-aminophosphonates catalyzed by recyclable nano-magnetic sulfated zirconia (Fe_3O_4@ZrO_2/SO_4^{2-}). RSC Adv., 2016, 6, 16046–16056. doi: 10.1039/C5RA13173A.

Ghose A.K., Viswanadhan V.N., Wendoloski J.J., Prediction of hydrophobic (lipophilic) properties of small organic molecules using fragmental methods: An analysis of ALOGP and CLOGP methods. J. Phys. Chem. A., 1998, 102, 3762–3772. doi: 10.1021/jp980230o.

Ghosh R., Maiti S., Chakraborty A., Maiti D. K., $In(OTf)_3$ catalysed simple one-pot synthesis of α-amino phosphonates. J. Mol. Catal. A: Chem., 2004, 210, 53–57. doi: 10.1016/j.molcata.2003.09.020.

Haji basha M., Subramanyam Ch., Prasada Rao K., Ultrasound-promoted solvent-free synthesis of some new α-aminophosphonates as potential antioxidants. Main group met. Chem., 2020, 43, 147–153. doi: 10.1515/mgmc-2020-0018.

Hay M., Thomas D. W., Craighead J. L., Economides C., Rosenthal J., Clinical development success rates for investigational drugs. Nature Biotechnol. 2014, 32, 40–51. doi: 10.1038/nbt.2786.

Herczegh P., Buxton T.B., McPherson J.C., Kova´cs-Kulyassa A., Brewer P.D., Sztaricskai F., et al., Osteo adsorptive bisphosphonate derivatives of fluoroquinolone antibacterials. J. Med. Chem., 2002, 45(11), 2338–2341. doi: 10.1021/jm0105326.

Hidalgo-Figueroa S., Ramirez-Espinosa J.J., Estrada-Soto S., Almanza-Pérez J. C., Román-Ramos R., Alarcón-Aguilar F.J., et al. Discovery of thiazolidine-2,4-dione/biphenylcarbonitrile hybrid as dual PPAR α/γ modulator with antidiabetic effect: *in vitro*, *in silico* and *in vivo* approaches. Chem. Biol. Drug Des., 2013, 81, 474–483. doi: 10.1111/cbdd.12102.

Hirschmann R., Smith A.B., Taylor C.M., Benkovic P.A., Taylor S.D., Guang-Fang X., et al., Synthesis and antifungal activity of novel chiral α-aminophosphonates containing fluorine moiety. Science, 1994, 265, 234–237. doi: 10.1002/cjoc.200690296.

Hollenberg P.F., Characteristics and common properties of inhibitors, inducers, and activators of CYP enzymes. Drug Metab. Rev., 2002, 34, 17–35. doi: 10.1081/dmr-120001387.

Huang S.M., Strong J.M., Zhang L., Reynolds K.S., Nallani S., Temple R., et al., New era in drug interaction evaluation: US Food and drug administration update on CYP enzymes, transporters, and the guidance process. J. Clin. Pharmacol., 2008, 48, 662–670. doi: 10.1177/0091270007312153.

Huang X.C., Wang M., Pan Y.M., Yao G.Y., Wang H. S., Tian X.Y., et al., Synthesis and antitumor activities of novel thiourea α-aminophosphonates from dehydroabietic acid. Euro. J. Med. Chem., 2013, 69, 508–520. doi: 10.1016/j.ejmech.2013.08.055.

Ibrar A., Sumera Z., Imtiaz K., Zainab S., Aamer S., Jamshed I. New prospects for the development of selective inhibitors of α-glucosidase based on coumarin-iminothiazolidinone hybrids: synthesis, in vitro biological screening and molecular docking analysis. J. Taiwan Inst. Chem. Eng. 2017, 81, 119–133. doi: 10.1016/j.jtice.2017.09.041.

Jean-Luc M., Phosphinate chemistry in the 21st century: A viable alternative to the use of phosphorus trichloride in organophosphorus synthesis. Acc. Chem. Res., 2014, 47, 77–87. doi: 10.1021/ar400071v.

Kaboudin B., Kazemi F., Hosseini N.K., A novel straightforward synthesis of α-aminophosphonates: one-pot three-component condensation of alcohols, amines, and diethylphosphite in the presence of $CuO@Fe_3O_4$ nanoparticles as a catalyst. Res. Chem. Intermed., 2017, 43(8), 4475–4486. doi: 10.1007/s11164-017-2890-y.

Kafarski P., Lejczak B., Aminophosphonic acids of potential medical importance. Curr. Med. Chem. Anticancer Agents, 2001, 1, 301–312. doi: 10.2174/1568011013354543.

Karimi-Jaberi, Z., Amiri, Md., One-pot synthesis of α-aminophosphonates catalyzed by boric acid at room temperature. Heteroatom Chem., 2010, 21(2), 96–98. doi: 10.1002/hc.20577.

Kaur J., Singh A., Singh G., Verma R.K., Mall R., Novel indolyl linked *para*-substituted benzylidene-based phenyl containing thiazolidienediones and their analogs as α-glucosidase inhibitors: synthesis, *in vitro*, and molecular docking studies. Med. Chem. Res., 2018, 27, 903–914. doi: 10.1007/s00044-017-2112-6.

Kawade D., Nitin J., Jadhav V., Girish K., Design synthesis and evaluation of novel thiazolidinedione derivatives as antidiabetic agents. Pharma Innov. J., 2017, 6(12), 390–398.

Kuemin M., Donk W.A., Structure-activity relationships of the phosphonate antibiotic dehydrophos. Chem. Commun., 2010, 46, 7694–7696. doi: 10.1039/c0cc02958k.

Kuznetsov Y.I., Kazanskaya G.Y., Tsirulnikova N.V., Aminophosphonate corrosion inhibitors for steel. Prot. Met., 2003, 39, 120–123. doi: 10.1023/A:1022986625711.

Laachachi A., Cochez M., Ferriol M., Leroy E., Lopez Cuesta J.M., Oget N., Influence of Sb_2O_3 particles as filler on the thermal stability and flammability properties of poly(methyl methacrylate) (PMMA). Polym. Degrad. Stabil., 2004, 85, 641–646. doi: 10.1016/j.polymdegradstab.2004.03.003.

Lewkowski J., Tokarz P., Lis T., Slepokura K., Stereoselective addition of dialkyl phosphites to di-salicylaldimines bearing the (*R*,*R*)-1,2-diaminocyclohexane moiety. Tetrahedron, 2014, 70, 810–816. doi: 10.1016/j.tet.2013.12.042.

Lipinski C.A., Lombardo F., Dominy B.W., Feeney P.J., Experimental and computational approaches to estimate solubility and permeability in drug discovery and development settings. Adv. Drug Del. Rev., 2001, 46, 3–26. doi: 10.1016/s0169-409x(00)00129-0.

Liu H., Iwasawa Y., Unique performance and characterization of a crystalline SbRe2O6 catalyst for selective ammoxidation of isobutane. J. Phys. Chem. B., 2002, 106, 2319–2329. doi: 10.1021/jp013729i.

Madhu Kumar Reddy K., Mohan G., Bakthavatchala Reddy N., Sravya G., Peddanna K., Grigory V.Z., et al., Synthesis, antioxidant activity and α-glucosidase enzyme inhibition of α-aminophosphonate derivatives bearing piperazine-1,2,3-triazole moiety. J. Heterocyclic Chem., 2021, 58, 172–181. doi: 10.1002/jhet.4157.

Madhu Kumar Reddy K., Peddanna K., Varalakshmi M., Bakthavatchala Reddy N., Sravya G., Grigory V.Z., et al., Ceric ammonium nitrate (CAN) catalyzed synthesis and α-glucosidase activity of some novel tetrahydropyridine phosphonate derivatives. Phosphorus Sulfur., 2019, 194, 812–819. doi: 10.1080/10426507.2018.1550641.

Maheshwara Reddy N., Poojith N., Mohan G., Mohan Reddy Y., Saritha V. K., Visweswara Rao P. et al., Green synthesis, antioxidant, and plant growth regulatory activities of novel α-Furfuryl-2-alkylaminophosphonates. ACS Omega, 2021, 6(4), 2934–2948. doi: 10.1021/acsomega.0c05302.

Maier L., Organic phosphorus compounds 91.[1] synthesis and properties of 1-amino-2-arylethylphosphonic and -phosphinic acids as well as -phosphine oxides. Phosphorus Sulfur., 1990, 53, 43–67. doi: 10.1080/10426509008038012.

Matsumura H., Okumura K., Shimamura T., Ikenaga N., Miyake T., Suzuki T., Selective oxidation of methane to formaldehyde over antimony oxide-loaded catalyst. J Mol Catal A., 2006, 250, 122–130. doi: 10.1016/j.molcata.2006.01.043.

Meyer J.H., Barlett P.A., Macrocyclic inhibitors of penicillopepsin: Design, synthesis, and evaluation of an inhibitor bridged between P1 and P3. J. Am. Chem. Soc., 1998, 120, 4600–4609. doi: 10.1021/ja973715j.

Miller D.J., Hammond S.M., Anderluzzi D., Bugg T.D.H., Aminoalkylphosphinate inhibitors of D-Ala-D-Ala adding enzyme. J. Chem. Soc. Perkin Trans., 1998, 1, 131–142. doi: 10.1039/A704097K.

Mitragotri S.D., Pore D.M., Desai U.V., Wadgaonkar P.P., Sulfamic acid: An efficient and cost-effective solid acid catalyst for the synthesis of α-aminophosphonates at ambient temperature, Catal. Commun., 2008, 9, 1822–1826. doi: 10.1016/j.catcom.2008.02.011.

Mohammadiyan E., Ghafuri H., Kakanejadifard A., A new procedure for synthesis of α-aminophosphonates by aqueous formic acid as an effective and environment-friendly organocatalyst.

J. Chem. Sci., 2017, 129, 1883–1891. doi: org/10.1007/s12039-017-1394-z.

Mohan G., Santhisudha S., Madhu Kumar Reddy K., Vasudeva Reddy N., Vijaya T., Suresh Reddy C., Phosphosulfonic acid-catalyzed green synthesis and bioassay of α-aryl-α′-1,3,4-thiadiazolyl aminophosphonates. Heteroatom Chem., 2016, 27, 1–10. doi: 10.1002/hc.21325.

Montanari F., Ecker G.F., Prediction of drug-ABC-transporter interaction-Recent advances and future challenges. Adv. Drug Deliv. Rev., 2015, 86, 17–26. doi: 10.1016/j.addr.2015.03.001.

Mori M., Takagi M., Noritake C., Kagabu S., 2,4-Dioxo-1,3-thiazolidine derivatives as a lead for new fungicides. J. Pestic. Sci., 2008, 33, 357–363. doi: 10.1584/jpestics.G08-15

Motevalli S., Iranpoor N., Etemadi-Davan E., Moghadam K.R. Exceptional effect of nitro substituent on the phosphonation of imines: the first report on phosphonation of imines to α-iminophosphonates and α-(*N*-phosphorylamino)phosphonates. RSC Adv., 2015, 5, 100070–100076. doi: 10.1039/C5RA14393D.

Mucha A., Kafarski P., Berlicki, L., Remarkable potential of the α-aminophosphonate/phosphinate structural motif in medicinal chemistry, J. Med. Chem., 2011, 54, 5955–5980. doi: 10.1021/jm200587f.

Muegge I., Heald S.L., Brittelli D., Simple selection criteria for drug-like chemical matter. J. Med. Chem., 2001, 44, 1841–1846. doi: 10.1021/jm015507e.

Nalin M., Messaddeq Y., Ribeiro S.J.L., Poulain M., Briois V., Photosensitivity in antimony based glasses. J. Optoelectron Adv. M., 2001, 3, 553–558.

Nanda K.K., Sahu S.N., Behera S.N., Liquid-drop model for the size-dependent melting of low-dimensional systems. Phys. Rev. A-At. Mol. Opt. Phys., 2002, 66, 132081. doi: 10.1103/PhysRevA.66.013208.

Natchev I.A., Synthesis, enzyme-substrate interaction, and herbicidal activity of phosphoryl analogues of lycine. Liebigs Ann. Chem., 1988, 9, 861–867. doi: 10.1002/jlac.198819880908.

Naydenova E.D., Todorov P.T., Troev, K.D., Recent synthesis of aminophosphonicacids as potential biological importance, Amino Acids, 2010, 38, 23–30. doi: 10.1007/s00726-009-0254-7.

Nickavar B., Amin G., Enzyme assay guided isolation of an alpha-amylase inhibitor flavonoid from vaccinium arctostaphylos leaves. Iran J. Pharm. Res., 2011, 10, 849–853. PMCID: PMC3813050.

Ningbo L., Wang X., Qiu Xu R., Chen X., Zhang J., Chen X., et al., Air-stable zirconocene bis(perfluorobutanesulfonate) as a highly efficient catalyst for synthesis of α-aminophosphonates via Kabachnik–Fields reaction under solvent-free condition. Cat. Comm., 2014, 43(5), 184–187. doi: 10.1016/j.catcom.2013.10.013.

Ordonez M., Cabrera H.R., Cativiela C., An Overview of stereoselective synthesis of α-aminophosphonic acids and derivatives. Tetrahedron., 2009, 65, 17–49. doi: 10.1016/j.tet.2008.09.083.

Orsini F., Sello G., Sisti M., Aminophosphonic acids and derivatives. Synthesis and biological applications. Curr. Med. Chem., 2010, 17(3), 264–289. doi: 10.2174/092986710790149729.

Ozawa K., Sakka Y., Amano M., Preparation and electrical conductivity of three types of antimonic acid films. J. Mater. Res., 1998, 13, 830–833. doi: 10.1557/JMR.1998.0107.

Patil V. S., Nandre K. P., Ghosh S., Rao V. J., Chopade B. A., Sridhar B., et al., Synthesis, crystal structure and anti-diabetic activity of substituted (E)-3-(benzo[d]thiazol-2-ylamino)phenylprop-2-en-1-one. Eur. J. Med. Chem., 2013, 59, 304–309. doi: 10.1016/j.ejmech.2012.11.020.

Pavan Phani Kumar M., Anuradha V., Subramanyam Ch., Hari Babu V.V., *In silico* molecular docking study, synthesis and α-amylase inhibitory activity evaluation of phosphorylated derivatives of purine. Phosphorus Sulfur., 2021, 196(11), 1010–1017. doi: 10.1080/10426507.2021.1960833.

Prashantha Kumar B.R., Soni M., Kumar S.S., Singh K., Patil M., Baig R.B.N., et al., Synthesis, glucose uptake activity and structure-activity relationships of some novel glitazones incorporated with glycine, aromatic and alicyclic amine moieties via two carbon acyl linker. Eur. J. Med. Chem., 2011, 46, 835–844. doi: 10.1016/j.ejmech.2010.12.019.

Quin L.D., Verkade J.G., Phosphorus-31 NMR Spectral Properties Compound Characterization and Structural Analysis; VCH Publishers: New York, 1994.

Ramandeep K., Rajnish K., Nilambra D., Ashok K., Ashok Kumar Y., Manoj K., Synthesis and studies of thiazolidinedione-isatin hybrids as α-glucosidase inhibitors for management of diabetes. Future Med. Chem. 2021, 13(5), 1–5. doi: 10.4155/fmc-2020-0022.

Ravikumar D., Mohan S., Subramanyam Ch., Prasada Rao K., Ultrasound-promoted greener approach to synthesize some new α-aminophosphonates catalyzed by nano $BF_3{\cdot}SiO_2$ under solvent-free condition and their antioxidant activity evaluation. Phosphorus Sulfur., 2018, 193(6), 400–407. doi: 10.1080/10426507.2018.1424163.

Ravikumar D., Subramanyam Ch., Mohan S., Prasada Rao K., Microwave assisted greener approach to synthesize α-aminophosphonates under catalyst free and solvent-free condition and their bioactivity evaluation. Int. J. Res. Eng. App. Manang., IMC18619(special issue), 2018, 327–333.

Rostamizadeh M., Maghsoodlou M. T., Hazeri N., Habibi-khorassani Sd. M., Keishams L., A novel and efficient synthesis of α-aminophosphonates by use of triphenyl phosphite in acetic acid media. Phosphorus Sulfur., 2011, 186(2), 334–337. doi: 10.1080/10426507.2010.500641.

Sahu S.K., Banerjee M., Mishra S.K., Mohanta R.K., Panda P.K., Misro P.K., Synthesis, partition coefficients and antibacterial activity of 3′-phenyl (substituted)-6′ aryl-2′ (1H)-cis-3′,3′a-dihydrospiro [3-H-indole-3,5'-pyrazolo (3′,4′-d)-thiazolo-2-(1H) ones]. Acta Pol. Pharm., 2007, 64(2), 121–126. PMID: 17665861.

Senthil Kumar N., Vijaya kumar V., Sarveswari S., Sarveshwari G.A., Gayathri M., Synthesis of new thiazolidine-2,4-dione-azole derivatives and evaluation of their α-amylase and α-glucosidase inhibitory activity. Iran J. Sci. Technol. Trans. Sci., 2019, 43, 735–745. doi: 10.1007/s40995-018-0593-x.

Shameem M.A., Orthaber A., Organophosphorus compounds in organic electronics. Chem-Eur J., 2016, 22, 10718–10735. doi: 10.1002/chem.201600005.

Shiro T., Fukaya T., Tobe M., The chemistry and biological activity of heterocycle-fused quinolinone derivatives: a review. Eur. J. Med. Chem., 2015, 97, 397–408. doi: 10.1016/j.ejmech.2014.12.004.

Smith W.W., Bartlett P.A., Macrocyclic inhibitors of penicillopepsin. 3. Design, synthesis, and evaluation of an inhibitor bridged

between P2 and P1. J. Am. Chem. Soc., 1998, 120, 4622–4628. doi: 10.1021/ja973713z.

Spengler J., Anderle F., Bosch E., Grasselli R.K., Pillep B., Behrens P., et al., Antimony oxide-modified vanadia-based catalysts physical characterization and catalytic properties. J. Phys. Chem. B., 2001, 105, 10772–10783. doi: 10.1021/jp012228u.

Sreekanth Reddy P., Vasu Govardhana Reddy P., Mallikarjun Reddy S., 2,4,6-Tris(4-iodophenoxy)-1,3,5-triazine as a new recyclable "iodoarene" for *in situ* generation of hypervalent iodine(III) reagent for α-tosyloxylation of enolizable ketones. Tetrahedron Lett., 2014, 55, 3336–3342. doi: 10.1016/j.tetlet.2014.04.052.

Subramanyam Ch., Taslim Bhasha S.K., Madhava G., Adam S.K., Srinivasa Murthy S.D., Naga Raju C., Synthesis, spectral characterization and bioactivity evaluation of novel α-aminophosphonates. Phosphorus Sulfur., 2017, 192(3), 267–270. doi: 10.1080/10426507.2016.1225056.

Sujatha B., Mohan S., Subramanyam Ch., Prasada Rao K., Microwave-assisted synthesis and anti-inflammatory activity evaluation of some novel α-aminophosphonates. Phosphorus Sulfur., 2017, 192(3), 267–270. doi: 10.1080/10426507.2017.1331233.

Sujatha B., Mohan, S., Subramanyam Ch., Prasada Rao K., Microwave-assisted synthesis and anti-inflammatory activity evaluation of some novel α-aminophosphonates. Phosphorus Sulfur., 2017, 192(3), 267–270. doi: 10.1080/10426507.2017.1331233.

Sujatha B., Mohan S., Subramanyam Ch., Prasada Rao K., Microwave-assisted synthesis and anti-inflammatory activity evaluation of some novel α aminophosphonates. Phosphorus Sulfur., 2017, 192(10), 1110–1113. doi: 10.1080/10426507.2017.1331233.

Sujatha B., Subramanyam Ch., Venkataramaiah Ch., Rajendra W., Prasada Rao K., Synthesis and anti-diabetic activity evaluation of phosphonates containing thiazolidinedione moiety. Phosphorus Sulfur., 2020, 195(7), 586–591. doi: 10.1080/10426507.2020.1737061.

Syama Sundar C., Bakthavatchala Reddy N., Sivaprasad S., Uma Maheswara Rao K., Jaya Prakash S.H., Suresh Reddy C., Tween-20: an efficient catalyst for one-pot synthesis of α-aminophosphonates in aqueous media. Phosphorus Sulfur., 2014, 189, 551–557. doi: 10.1080/10426507.2011.631641.

Syamala M., Recent progress in three-component reactions. An update. Org. Prep. Proced. Int., 2009, 41, 1–68. doi: 10.1080/00304940802711218.

Tanaka, K.F., Solvent-free organic synthesis. Chem. Rev., 2000, 100, 1025. doi: 10.1021/cr940089p.

Tang J., Wanga L., Wang W., Zhang L., Wu S., Mao D., A facile synthesis of α-aminophosphonates catalyzed by ytterbium perfluorooctanoate under solvent-free conditions. J. Fluor. Chem., 2011, 132, 102–106. doi: 10.1016/j.jfluchem.2010.12.002.

Trott O., Olson A.J., AutoDock Vina: improving the speed and accuracy of docking with a new scoring function, efficient optimization and multithreading. J. Comput. Chem., 2010, 31, 455–461. doi: 10.1002/jcc.21334.

Vahdat S. M., Baharfar R., Tajbakhsh M., Heydari A., Baghbanian S. M., Haksar S., Organocatalytic synthesis of α-hydroxy and α-aminophosphonates. Tetrahedron Lett., 2008, 49, 6501–6504. doi: 10.1016/j.tetlet.2008.08.094.

Veber D.F., Johnson S.R., Cheng H.Y., Smith B.R., Ward K.W., Kopple K.D., Molecular properties that influence the oral bioavailability of drug candidates. J. Med. Chem., 2002, 45, 2615–2623. doi: 10.1021/jm020017n.

Vijay M.P., Kalpana N.T., Neha M.U., Ramaa C.S., Synthesis, *in-vitro* evaluation and molecular docking study of *N*-Substituted thiazolidinediones as α-glucosidase inhibitors. Chem. Select. 2022, 7, 1–11. doi: 10.1002/slct.202103848.

Vorathavorn V. I., Sykes J. E., Feldman D. G., Vet J., Cryptococcosis as an emerging systemic mycosis in dogs. J. Vet. Emerg. Crit. Care, 2013, 23, 489–497. doi: 10.1111/vec.12087.

Wang A., Xu Y., Gao Y., Huang Q., Luo X., An H., et al., Chemical and bioactive diversities of the genera Stachybotrys and Memnoniella secondary metabolites. Phytochem. Rev., 2015, 14, 623–655. doi: 10.1007/s11101-014-9365-1.

Wang G., Peng Y., Xie Z., Wang J., Chen M., Synthesis, α-glucosidase inhibition and molecular docking studies of novel thiazolidine-2,4-dione or rhodanine derivatives. Med. Chem. Comm., 2017, 8, 1477–1484. doi: 10.1039/c7md00173h.

Xie C.S., Hu J.H., Wu R., Xia H., Structure transition comparison between the amorphous nanosize particles and coarse-grained polycrystalline of cobalt. Nanostruct. Mater., 1999, 11(8), 1061–1066.

Xie D., Zhang A., Liu D., Yin Wan J., Zeng S., et al., Synthesis and antiviral activity of novel α-aminophosphonates containing 6-fluorobenzothiazole moiety. Phosphorus Sulfur., 2017, 192, 1061–1067. doi: 10.1080/10426507.2017.1323895.

Xie X.L., Li R.K.Y., Liu Q.X., Mai Y.W., Structure-property relationships of *in-situ* PMMA modified nano-sized antimony trioxide filled poly(vinyl chloride) nanocomposites. Polymer, 2004, 45, 2793–2802. doi: 10.1016/j.polymer.2004.02.028.

Yang S., Gao X.W., Diao C.L., Song B., Jing L.H., Xu G.G., et al., Synthesis and antifungal activity of novel chiral α-aminophosphonates containing fluorine moiety. Chinese J. Chem., 2006, 24, 1581–1588.

Yoshioka T., Fujita T., Kanai T., Aizawa Y., Kurumada T., Hasegawa K., et al., Studies on hindered phenols and analogues.1-Hypolipidemic and hypoglycemic agents with ability to inhibit lipid peroxidation. J. Med. Chem., 1989, 32(2), 421–428. doi: 10.1021/jm00122a022

Young M.H., Yun Jung P., Jin-Ah K., Daeui P., Ji Young P., Hye Jin L. et al., Design and synthesis of 5-(substituted benzylidene) thiazolidine-2,4-dione derivatives as novel tyrosinase inhibitors. Eur. J. Med. Chem., 2012, 49, 245–252. PMID 22301213.

Yu Y.Q., Xu D.Z., A Simple and green procedure for the one-pot synthesis of α-aminophosphonates with quaternary ammonium salts as efficient and recyclable reaction media. Synthesis, 2015, 47, 1869–1876. doi: 10.1055/s-0034-1380523.